Extended description for electron capture in ion-atom collisions: Application of model potentials within the framework of the continuum-distorted-wave theory

L. Gulyás,[1,2] P. D. Fainstein,[3] and T. Shirai[2]
[1]*Institute of Nuclear Research of the Hungarian Academy of Sciences (ATOMKI), P.O. Box 51, H-4001 Debrecen, Hungary*
[2]*Japan Atomic Energy Research Institute, Kizu-cho, Kyoto 619-0215, Japan*
[3]*Centro Atómico Bariloche, Comisión Nacional de Energía Atómica, Avenida E. Bustillo 9500, 8400 Bariloche, Argentina*
(Received 12 March 2001; revised manuscript received 3 August 2001; published 8 May 2002)

We perform an extension of the continuum-distorted-wave (CDW) approximation for single electron capture by introducing model potentials to describe the interaction of the active electron with the residual-target and projectile ions. The cross sections for electron transfer in collisions of bare and dressed projectile ions with H and He atoms are calculated and compared with experimental data and previous CDW calculations that make use of approximate analytical wave functions to represent the active electron initial and final states. For electron capture in proton-He collisions into definite final states the present calculations are in better agreement with experiments. We trace the differences in the results from both models to a different behavior at projectile scattering angles close to the Thomas peak. In the case of dressed projectiles with different charge states impinging on H and He the present version of CDW gives a better representation of the filling of the unoccupied orbitals of the dressed ion and, therefore, of the cross section as a function of the impinging ion charge state.

DOI: 10.1103/PhysRevA.65.052720 PACS number(s): 34.70.+e

I. INTRODUCTION

The study of electron capture in ion-atom collisions has been considerably advanced during the last decades (e.g., reviews in Refs. [1–3]). Of particular interest are the medium and high impact energy domains where perturbative approaches provide a good account of the process.

The roles of different mechanisms leading to charge transfer, such as energy resonance, single and double scattering of the captured electron, etc., were explored in detail during the 1970s. However, almost all theoretical studies have been carried out for the simplest three-body system. On the contrary, experiments have nearly exclusively been done on multielectron collision systems [1,3] and only a few on simple systems.

Different methods have been developed to extend three-body models to more complicated systems. The first attempts were done using the independent electron model (IEM) [1], where a given ''active'' electron is assumed to evolve independently of the others in the Coulomb field of colliding heavy nuclei screened by a static potential of the other ''passive'' electrons. The main limitation of IEM lies in the inclusion of electron-electron interaction, and so the model is expected to provide a good description of the collision process where the correlated motion of the electrons are negligible in the collision [4]. At the same time as it is well known that it is very difficult to treat the many-electron problem when all interactions are included in the calculation. Such treatment allows one to study in detail the effect of the electron-electron correlation, and, therefore, to test the approximations introduced in the independent electron model [4]. Among the very few studies along this direction [4] more recently the continuum-distorted-wave (CDW) model has been devised to include all interactions in the four-body treatment [5–7]. Two active electrons are included in the calculation, which allows one to study the effects of electron-electron interaction in single and double transfer and transfer ionization processes. However, an extension of this scheme to more complicated systems in which both the projectile and target have many electrons, seems outside our present capabilities. Therefore, we have chosen to use the independent electron model with the most accurate single-particle model potentials to represent the interaction between the active electron and the screened many-electron projectile and target. While this method neglects dynamical correlation and takes into account only to a certain extent the static correlation, it allows one to study in a single framework the cases of multielectronic targets and of dressed projectiles.

As indicated above a crucial ingredient of the independent electron model are the model potentials used to represent the many electronic target and projectile. However, the description of the static potentials usually involves additional approximations in the applications of the model. One of the most essential approximations lies in considering the general collisions process where both the projectile and target bring electrons into the collisions and the static field on one of the collision partners, usually the projectile, has been described by a simple Coulomb field with effective charge, while the averaged potential based on the Hartree-Fock scheme has often been employed for the other partner. This means that the interaction between active and passive electrons has been treated asymmetrically in the incoming and outgoing channels [3]. Of course such restrictions were reasonable in the earlier application of more involved three-body theories, such as the CDW model. However, it is obvious that, if the field of passive electrons has been poorly approximated, or if these fields have inconsistently been used in the different collision channels, it might considerably affect the actual values of the calculated quantities. This makes the judgment on the validity criteria for the application of the three-body model and IEM very difficult. Therefore, in those processes

where there remain discrepancies between experiment and theory the following question arises: are the discrepancies due to the electron correlation effect or are they related to some shortcomings of additional approximations introduced on top of the IEM? In our days the computational facilities makes it feasible, as it will be shown here, to apply the IEM to a collision where the fields statics electron both on the projectile and target are represented in a more accurate way. In this case the interaction between the projectile and the target electrons will greatly differ with respect to that of a bare ion, specially at small distances where the reaction takes place.

In this work we will employ the perturbative CDW model within the framework of the independent electron model, taking particular care to represent the target and projectile bound and continuum wave functions in the most accurate form. With this objective we will extend the continuum-distorted-wave model for single-electron capture to the most general case of collisions between multielectron (or dressed) ions and atoms within the framework of the independent electron model.

The CDW model [8,9] is one of the most successful models at medium and high impact energies. It belongs to a family of multiple scattering approaches and includes contributions from higher-order scattering terms in the conventional Born series [3]. Despite a few deficiencies discussed in Ref. [10] the CDW model has major advantages: (i) it accounts for the long-range behavior of the Coulomb potential and includes distortions in the entrance and exit channels on equal footing, (ii) the scattering amplitude is given analytically in the case of Coulomb potentials and if the wave functions are developed in a linear combination of Slater-type orbitals [1,3], (iii) the model gives reasonable agreement with experiments for a number of collision systems. In the case of multielectronic targets, except the very recent application of four-body collisions, the model has been limited by the use of Coulomb potential with an effective charge to describe the distortion by the residual-target ion. In the present extension of CDW the potential due to the projectile and target nuclei and the passive electrons bound to them are represented by spherically symmetric model potentials in both the initial and final channels. Therefore, the active electron evolves in a two-center potential defined by these two model potentials. This allows for a more accurate description of the initial-target and final-projectile bound states and of the distortions in both channels. Similar extension of the CDW and symmetric Eikonal models have already been achieved for ionization [11] and excitation [12], respectively. For electron capture, a scheme to go beyond the limitation of Coulomb distortion by the target ion was proposed by Bachau *et al.* [13]. However, their extension is not easy to apply as it based on analytic expression of numerical wave functions. The present application goes also beyond this limitation.

The layout of the paper is as follows. We will discuss the extension of the CDW model to the collisions between multielectron targets and dressed ions in Sec. II. In Sec. III, the results for single electron capture in collisions between H^+ and $A^{(2-5)+}$ with H and He targets are presented and the role of screening by the passive electrons is discussed. Conclusions are drawn in Sec. IV. Atomic units are used, unless otherwise stated.

II. THEORY

Let us consider the transfer of one electron from the target atom B to a projectile ion A^{q+} with charge $q+$,

$$A^{q+}+(e-B^+)\rightarrow A^{(q-1)+}+B^+. \tag{1}$$

Here one electron from B is supposed to be captured independently of the other electrons, that is, the former is active and the latter (passive) remain frozen during the collision. We adopt here the semiclassical treatment where the heavy projectile moves along a linear trajectory, so that the electronic Hamiltonian is given as

$$H=-\frac{1}{2}\nabla_r^2+V_A(\boldsymbol{s})+V_B(\boldsymbol{x}), \tag{2}$$

where $\boldsymbol{s}$, $\boldsymbol{x}$, and $\boldsymbol{r}$ denote the position vectors of the active electron with respect to a reference frame fixed at A^{q+}, B^+ and to the midpoint of the internuclear separation A^{q+}-B^+. The potential V_A (V_B) describes the interaction between the active electron and A^{q+} (B^+). In Eq. (2) we neglect the internuclear interaction since it plays no role for the total cross sections or the differential cross sections at small scattering angle that we will study here [1].

In the three-body formulation of the CDW model the distorted waves are introduced as follows [8,9]:

$$\begin{aligned}\xi_i^+ &= \varphi_i(\boldsymbol{x})E_{i,-\boldsymbol{v}}(\boldsymbol{r})N(\nu_A)\,{}_1F_1(i\nu_A;1;iv s+i\boldsymbol{v}\cdot\boldsymbol{s})\\ &= \varphi_i(\boldsymbol{x})E_{i,-\boldsymbol{v}}(\boldsymbol{r})D^+_{-\boldsymbol{v}}(Z_A,\boldsymbol{s})\\ &= \varphi_i(\boldsymbol{x})E_{i,-\boldsymbol{v}}(\boldsymbol{r})\exp(i\boldsymbol{v}\cdot\boldsymbol{s})\psi^+_{-\boldsymbol{v}}(Z_A,\boldsymbol{s}),\end{aligned} \tag{3}$$

$$\begin{aligned}\xi_f^- &= \varphi_f(\boldsymbol{s})E_{f,\boldsymbol{v}}(\boldsymbol{r})N(\nu_B)\,{}_1F_1(-i\nu_B;1;-iv x-i\boldsymbol{v}\cdot\boldsymbol{x})\\ &= \varphi_f(\boldsymbol{s})E_{f,\boldsymbol{v}}(\boldsymbol{r})D^-_{\boldsymbol{v}}(Z_B,\boldsymbol{x})\\ &= \varphi_f(\boldsymbol{s})E_{f,\boldsymbol{v}}(\boldsymbol{r})\exp(-i\boldsymbol{v}\cdot\boldsymbol{x})\psi^-_{\boldsymbol{v}}(Z_B,\boldsymbol{x}),\end{aligned} \tag{4}$$

with

$$E_{n,\boldsymbol{u}}=\exp\left[i\frac{1}{2}\boldsymbol{u}\cdot\boldsymbol{r}-i\frac{1}{8}u^2t-i\epsilon_n t\right], \tag{5}$$

where $\boldsymbol{v}$ is the collision velocity, ${}_1F_1$ denotes the hypergeometric function, and $\epsilon_{i,f}$ are the binding energies of the active electron in the initial and final states. In this way the initial (final) distorted wave function represents an initial (final) bound state distorted by a multiplicative factor that takes into account the fact that the active electron is simultaneously in a continuum state of the projectile (residual target) ion. These factors ensure that the initial and final distorted waves satisfy the correct asymptotic conditions for long-range potentials. The bound φ and continuum ψ wave functions are solutions of the equations

$$\left(-\frac{1}{2}\nabla_{x,s}^2+V_X-\epsilon_{i,f}\right)\varphi_{i,f}=0, \tag{6}$$

$$\left(-\frac{1}{2}\nabla_{x,s}^2+V_X-v^2\right)\psi_{\boldsymbol{v}}^{+}=0 \tag{7}$$

with $\nu=Z_X/v$, Z_X denotes the charge of nucleus X (X stands for A or B) and $N(\nu)=\exp(\nu\pi/2)\Gamma(1-i\nu)$. The distorted waves (3) and (4) satisfy the equation

$$\left(H-i\frac{\partial}{\partial t}\right)\xi_{i,f}^{\pm}=-(\boldsymbol{\nabla}_s\cdot\boldsymbol{\nabla}_x)\xi_{i,f}^{\pm}, \tag{8}$$

where the right-hand side defines the channel perturbative potential. The first-order approximation to the transition amplitude as a function of the impact parameter $\boldsymbol{\rho}$ is given by

$$T_{i,f}(\boldsymbol{\rho})=-i\int_{-\infty}^{+\infty}dt\left\langle \xi_f^{-}\left|H-i\frac{d}{dt}\right|\xi_i^{+}\right\rangle, \tag{9}$$

which, using the well-known method of Fourier transform, can be cast in the form [1,14]

$$T_{if}(\boldsymbol{\eta})=-N(\nu_A)N(\nu_B)\boldsymbol{I}_A\cdot\boldsymbol{J}_B, \tag{10}$$

where $\boldsymbol{\eta}$ is the transverse component of the projectile momentum transfer and $\boldsymbol{I}_A$ and $\boldsymbol{J}_B$ are defined as follows:

$$\boldsymbol{I}_A=\int d\boldsymbol{s}\exp(i\boldsymbol{\rho}_A\cdot\boldsymbol{s})\varphi_f^{*}(\boldsymbol{s})\boldsymbol{\nabla}_s D_{\boldsymbol{v}}^{+}(Z_A,\boldsymbol{s}), \tag{11}$$

$$\boldsymbol{J}_B=\int d\boldsymbol{x}\exp(i\boldsymbol{\rho}_B\cdot\boldsymbol{x})D_{-\boldsymbol{v}}^{-}(Z_B,\boldsymbol{x})\boldsymbol{\nabla}_x\varphi_i(\boldsymbol{x}), \tag{12}$$

with

$$\boldsymbol{\rho}_{A,B}=\pm\boldsymbol{\eta}-\left(\frac{v}{2}\pm\frac{\epsilon_i-\epsilon_f}{v}\right)\hat{\boldsymbol{v}}, \tag{13}$$

where the $+(-)$ sign corresponds to the label A (B). The total cross section for electron capture is obtained from

$$\sigma_{if}=(2\pi v)^{-2}\int d\boldsymbol{\eta}|T_{if}(\boldsymbol{\eta})|^2. \tag{14}$$

In the above formulation of the CDW model the interaction potentials V_A and V_B were taken as Coulomb potentials. Therefore, the bound-state wave functions are hydrogenic wave function and the distortion functions $D_{\boldsymbol{v}}^{\pm}$ are related to the Coulomb continuum wave functions $\psi_{\boldsymbol{v}}^{\pm}$ describing the electron as moving with velocity $\boldsymbol{v}$ in the field produced by the target or the projectile ions. In such cases the integrals in Eqs. (11) and (12) are given in analytic closed forms. This is a great advantage in the application of the theory because it allows for a very fast calculation of the cross sections.

The extension of the CDW model to multielectron targets and dressed projectiles requires model potentials that take into account the departure from the Coulomb potential at small distances. The first step in this direction was taken by Belkić *et al.* [1], by using the Roothaan-Hartree-Fock wave functions from Clementi and Roetti [15] for the bound electron in the initial state and a Coulomb function with an effective charge for the continuum distortion on the captured electron by the residual target ion [see Eq. (4)]. This extension of the model aims at obtaining an analytic expression of the transition amplitude, however, at the expense of using different potentials for the interaction of the active electron with the target ion (e-B^+) in the initial and final channels. Bachau *et al.* [13] modified this model by solving the Schrödinger equations (6) and (7) numerically with the same model potential for the electron-target ion interaction in both the initial and final channels. In practice, the continuum wave functions (7) were expanded in terms of Slater-type orbitals so that the integral (12) was calculated analytically. At higher energies, however, the continuum wave functions have to be expanded over a large set of Slater-type orbitals to get converged results. This fact makes the method very impractical.

In this work we follow the ideas of Bachau *et al.* [13]: the wave functions are calculated using a model potential, with the exception that the expansion of continuum wave functions over Slater-type orbitals is avoided. The integral $\boldsymbol{I}_A$ can be transformed into the forms

$$\boldsymbol{I}_A=i\boldsymbol{\rho}_A I_{A1}(\boldsymbol{\rho}_A)+\boldsymbol{I}_{A2}(\boldsymbol{\rho}_A), \tag{15}$$

where

$$I_{A1}=\int d\boldsymbol{s}\exp(i\boldsymbol{\rho}_A\cdot\boldsymbol{s})\varphi_f^{*}(\boldsymbol{s})D_{\boldsymbol{v}}^{+}(Z_A,\boldsymbol{s}), \tag{16}$$

$$\boldsymbol{I}_{A2}=\int d\boldsymbol{s}\exp(i\boldsymbol{\rho}_A\cdot\boldsymbol{s})D_{\boldsymbol{v}}^{+}(Z_A,\boldsymbol{s})\boldsymbol{\nabla}_s\varphi_f^{*}(\boldsymbol{s}). \tag{17}$$

It is clear from these formulas that the integrals $\boldsymbol{I}_A$ and $\boldsymbol{J}_B$ can be evaluated in a similar manner. This is very convenient when the wave functions are given numerically and one can apply the methods developed in previous works [11,12]. Such circumstance offers and enables us to extend the model to collision systems involving multielectronic targets and also dressed projectile ions. Therefore, hereafter we can consider collision systems where one active electron of the target is transferred to the dressed ion. The electrons in the dressed ion are treated as frozen during the collision. The interaction between the active electron and the dressed projectile is represented by a model potential that takes into account the short-range interaction due to the passive electrons and the long-range shielding of the nuclear potential. There are a number of models to express an average field by such passive electrons in atoms and ions [3]. In the present work we have employed a Hartree-Fock-Slater (HFS) potential [16] for the target (V_B) and the model potentials from Szydlik and Green [17] for the dressed ion (V_A).

For the calculations of integrals I_{A1}, $\boldsymbol{I}_{A2}$, and $\boldsymbol{J}_B$, we apply the same procedures as in the previous studies for the ionization and excitation processes [11,12]. Namely, the bound states

$$\varphi(\boldsymbol{r}) = \frac{u_{nl}(r)}{r} Y_l^m(\hat{\boldsymbol{r}}), \tag{18}$$

characterized by the quantum numbers (nlm) and binding energy ϵ, and the continuum wave function

$$\psi_\epsilon^-(\boldsymbol{r}) = \frac{1}{r\sqrt{v}} \sum_{lm} i^l \exp(-i\delta_l) u_{\epsilon l}(r) [Y_l^m(\hat{\boldsymbol{r}})]^* Y_l^m(\hat{\boldsymbol{v}}) \tag{19}$$

with energy $\epsilon = v^2/2$, are obtained from the numerical solution of the Schrödinger equations (6) and (7), respectively. The details of the computational procedures for calculating Eqs. (12), (16), and (17) are not described here as they were given in Refs. [11] and [12]. Here we mention only about the slow convergence in the calculations connected to the partial-wave expansion (19). Such a difficulty usually occurs at high impact energies, especially at the values of momentum transfer that are related to the active electron double scattering [3]. In this region the numerical calculation becomes time consuming and unstable because the number of partial waves necessary for good convergence becomes very large. We have overcome this difficulty by adopting the ϵ algorithm [18], which was used to accelerate the convergence of the series expansion of continuum wave functions (19) in the numerical computation of the integrals (12), (16), and (17).

The present CDW code has been checked by calculating the total charge-transfer cross sections (14) in the H^+-$H(n_i l_i m_i) \rightarrow H(n_f l_f m_f)$-$H^+$ and H^+-$Ne(n_i l_i m_i) \rightarrow H(n_f l_f m_f)$-$Ne^+$ collisions. The quantum numbers $(n_i l_i m_i)$ and $(n_f l_f m_f)$ characterize the bound-state orbitals in the target and projectile spherical potentials, respectively. The calculated values are in good agreement in the whole energy range with the tabulated results of Belkić *et al.* [19] for H target. In the case of Ne, good agreement has also been obtained with the results of Bachau *et al.* [13] at 100-keV impact energy. However, at 300 keV slight discrepancies (10%–20%) have been observed, which might be due to the fact that only a small number of partial waves were included by Bachau *et al.* It must be noted that for this comparison we used the same potential as published in their paper. Results for single-electron transfer in the Be^{q+}-He collision were already reported in Ref. [20].

III. RESULTS AND DISCUSSION

A. Target distortion in the final state: A study of bare ions colliding with a He target

The main drawback of previous calculations with the CDW model (labeled hereafter CDW-H) is the use of different model potentials for the target atom in the initial and final channel. In the earlier work by Belkić *et al.* [1,14] the potential in the exit channel was approximated by a Coulomb potential with an effective nuclear charge obtained from the initial-state binding energy using the well-known formula for the hydrogen atom. This potential represents a kind of mean value at small distances, where the collision takes place, but misses the fine details of the potential and does not reproduce the correct asymptotic behavior of the potential, which corresponds to that of a singly charged ion. To explore the role of the residual-target potential in the final state we have chosen the simplest collision systems: a bare projectile ion colliding with a He atom. In our present work we will use for He the HFS potential [16] in both the incoming and outgoing channels (the CDW results obtained in this way will be referred to as CDW-HFS).

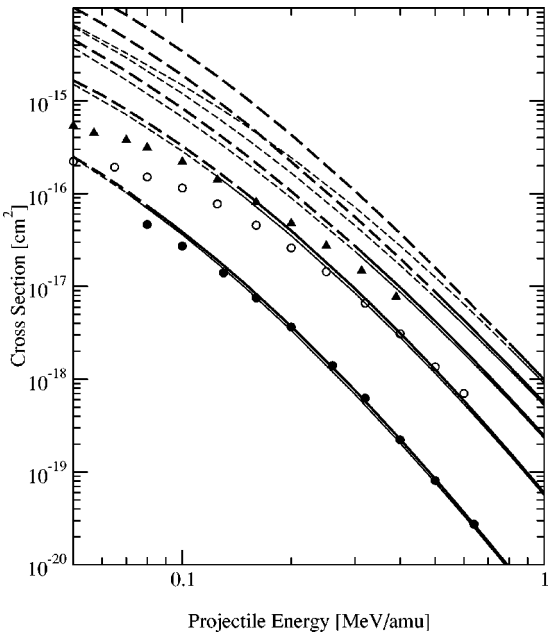

FIG. 1. Cross section for electron capture from He by bare ion impact. The curves from bottom to top refer to projectile charges from 1 to 5. Thick lines, present results (CDW-HFS); thin lines, CDW-H [14]. The lines are drawn as dashed in a region that lies outside the validity of the CDW model (see the text). ●, ○, and △ are experimental data, respectively, for H^+, He^{2+}, and Li^{3+} projectiles [21].

The validity of the replacement of the electron-residual-target interaction by a pure Coulomb potential depends on the process under study. The failure is most evident in the case of ionization, where the ejected electron usually moves for long time in the equipotential force created by the projectile and target ions (two-center effects [11]). In the case of excitation, on the other hand, the electron remains bound to the target and feels a much stronger field by a single (target) center [12]. Therefore, an accurate description of the initial ground state and of the final excited states is required. Interestingly, a similar effect can be observed in the case of electron capture. Figure 1 shows that the two treatments, CDW-H and CDW-HFS, provide almost identical total ($\sigma = \Sigma_f \sigma_{n_f l_f m_f}$) cross-section values in the energy region where the CDW model is expected to give accurate results. The validity criteria of CDW, which was determined empirically from the study of H^+-H, He collisions, can be given by the formula: E_P (keV/amu) $\geqslant$ 80 keV sup$\{|\epsilon_i|, |\epsilon_f|\}$ [1]. As this criteria is mostly based on a comparison between the binding energies and the impact energy one can expect that it will also hold for more complex systems. Namely, as in our pre-

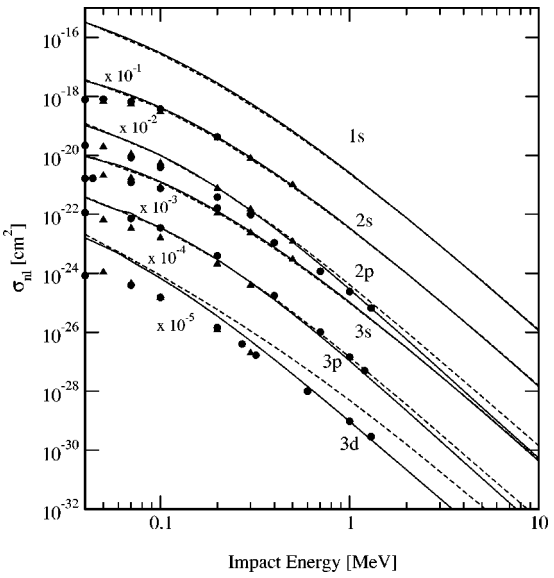

FIG. 2. Electron capture cross section for H^+-He collisions, as a function of projectile energy. Solid lines, present results (CDW-HFS); dashed lines, CDW-H results from [14]; ●, recommended data [26]; △, recommended data by Hoekstra *et al.* [25].

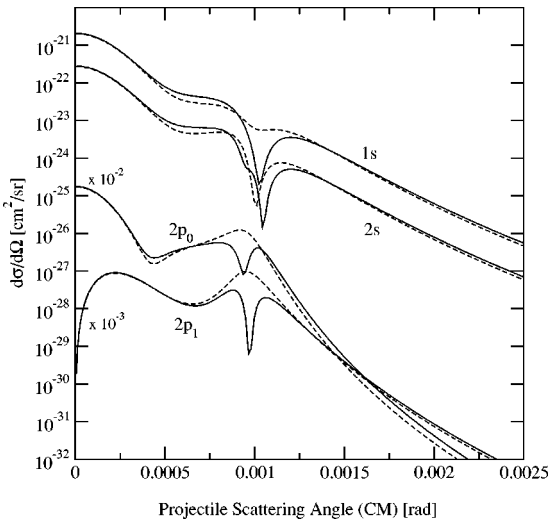

FIG. 3. Differential cross section plotted against the center-of-mass scattering angle of projectile in 1 MeV H^+-He$(1s)$ $\rightarrow H^+(nlm)+He^+(1s)$ collisions. Solid lines, present results; dashed lines, CDW results from [14].

vious work on the Be^{q+}-He collisions [20], we refer to this formula for estimating the validity region of CDW, when the model is applied to collisions with dressed projectiles (see later). In Fig. 1 the one-electron capture cross sections, available from the experiment of Shah and Gilbody [21], have also been presented. Good agreement can be observed with both the CDW-H and CDW-HFS calculations in the region where the models are expected to give realistic results.

The good agreement between the two theoretical treatments for describing total cross sections does not mean similar agreement in case of partial cross sections ($\sigma_{n_f l_f}$). This is well demonstrated by Fig. 2 for H^+-He collision, where a clear difference appears in the partial cross sections with increasing impact energies, especially on those with large l_f values.

The reason can readily be understood by investigating the differential cross section with respect to the projectile scattering angle. Figure 3 illustrates the result for 1-MeV impact energy. It is seen that the largest deviation between CDW-H and CDW-HFS appears at around the critical, Thomas-scattering angle of projectile ($\cong 0.001$ rad) associated with the successive, double scattering of the active electron on the projectile and target nuclei, respectively. This mechanism dominates the cross section at asymptotic impact velocities when capture between low-lying states are considered [3]. However, double scattering contributes dominantly even at moderate impact velocities if the electron is transferred to non-*s* or Rydberg states [22]. This occurs in the H^+-He collision at above a few hundred keV and 1-MeV impact energies when the electron is captured into the $3d$ and $2p$ orbitals, respectively. At the Thomas-scattering angle the CDW model produces an unphysical dip structure due to the interference between the distortions in the initial and final channels [23]. This splitting of the Thomas peak is a failure of the first-order CDW theories, such as CDW-HFS and CDW-H, as it has been demonstrated by Crothers and McCann [24] by performing a second-order CDW calculation where the dip, in agreement with the experimental results, does not appear. In a very recent work Belkić [7] studied other possibility of electron double scattering (first on the projectile and second on another target electron) and found that this mechanism produces also the Thomas peak in the differential scattering. This peak is so intensive as the one from the scattering on the projectile and on the target nuclei and does not show splitting of the Thomas peak at the critical scattering angle. The splitting of the Thomas peak, which is the case for homonuclear and heteronuclear collisions, is clearly seen for all the states studied by the present CDW model (see Fig. 3). As depicted by the dashed lines in the figure, however, such a dip disappears or is less pronounced in the CDW-H calculations [14]. So it is clear that the occurrence of the dip, although unphysical, depends strongly on the method for considering the interaction between the electron and the residual-target ion in a first-order CDW treatment. Figures 2 and 3 show that the discrepancies between the different treatments become evident in the integrated cross sections ($\sigma_{n_f l_f m_f}$) only in the case where the electron double scattering is the dominant mechanism. In such case the present CDW-HFS calculations are in better agreement with the recommended values based on experimental data [25,26], than the CDW-H results from [14] (see Fig. 2). Note that the recommended values are obtained from the analysis of those experimental data where the final state of the target was not observed, however, it can be found that inclusion of multiple processes would not increase the capture cross sections for the H^+-He reaction by more than 5% [1]. It is obvious that the first-order CDW models, such as CDW-HFS and CDW-H are not suitable for analyzing the differential capture cross sections, especially in the region of Thomas scattering. So the aim of the above analysis was only to study the origin of differences observed between the partial capture cross sections obtained from CDW-HFS and CDW-H models, respec-

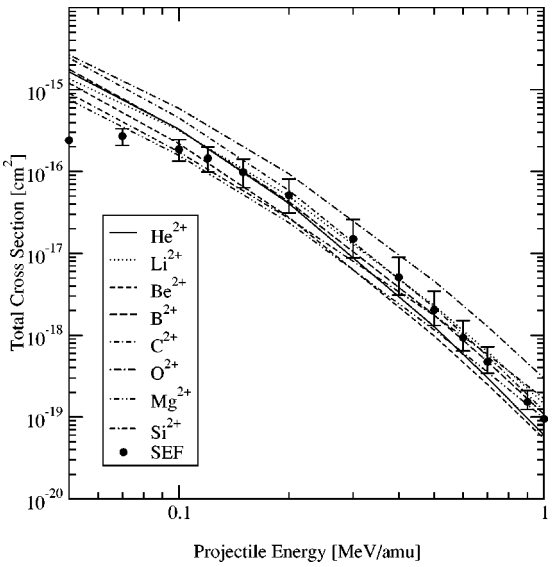

FIG. 4. Single electron capture cross sections in A^{2+}-He($1s$) $\rightarrow A^{+}$-He^{+}($1s$) collisions. Lines, present results; symbols are recommended data [27].

tively. This difference results from treating the electron-target interaction, which is very important in the Thomas mechanism. In the present CDW-HFS calculation the interaction between the active electron and target core is described on the same level both in the initial and final channels. This is consistent with the treatment of the capture process in the pure three-body case (proton-hydrogen collision), where the exact solutions for the Coulomb potential are used, and in spite of the splitting of the Thomas peak in the differential cross section the model provides a good account of the experimental total and partial cross sections [1].

B. Collisions of multiply charged dressed ions with H and He

Previous treatments of the CDW model only allowed one to consider bare projectile ions. The present extension allows to consider any dressed projectile such that the interaction between the ion and the active electron is represented by a model potential. In order to take into account the screening of the projectile nuclear charge by the passive electrons we have employed, for the different multiply-charged ions, the potentials given by Szydlik and Green [17]. Such a description of the projectile ion enables a more accurate calculation of wave functions and binding energies than the ones using a Coulomb field with effective charge. The electrons on the projectile were taken into account not only by their screening role. This electrons, due to the shell structure, occupy certain number of orbitals into which the active electron cannot be transferred (Pauli blocking). Test calculations show that the Pauli blocking has a crucial importance in the present treatment (see discussion below for A^{2+} ions).

1. A^{2+}-He collision

Figure 4 presents results for the calculation of single electron capture from He by selected doubly charged ions from He^{2+} to Si^{2+}. For comparison, the dots with error bars are the cross-section values evaluated from a semiempirical formula (SEF) derived by least-squares fits to experimental data [27]. The present predictions agree within the error bars with the recommended data for a number of projectile ions at above 100-keV/amu impact energies, where the CDW model is expected to provide realistic cross sections. However, for some cases, the present predictions deviate appreciably from the ones based on SEF. The recommended data rely on such experimental results which are obtained from measurements where the final state of the target ions were not observed. A study for the He^{2+}-He collision system shows that the contribution of multiple processes to the single electron capture channel [21], which is calculated by the present theory, do not contribute more than 10–20 %. We are not aware of other studies on whether such contribution is higher or lower for collisions with projectiles bringing electron into the collisions. Moreover, the semiempirical scaling formula is based on the assumption that the passive electron does not affect the process at all [28]. This assumption was useful to derive scaling laws with respect to the net charge q [2,27,29]. However, it is obvious that such scaling laws are less valid for the collisions with lowly ionized ions, especially for those with net charges $q \leqslant 2$ [28,29]. In the case of projectiles with low q the outermost electrons are less tightly bound, so electronic structure, differences in binding energies, etc., become more emphasized in the mechanism than they are for ions with high q. This is why we observe significant differences between cross sections for the different A^{2+} ions (see Fig. 3). From this point of view the above agreements/disagreements found between SEF and the theoretical results for different A^{2+} ions can be interpreted as accidental and so the comparison has only a qualitative meaning; however, we think such a comparison will stimulate further studies in the field.

Here, we also mention the crucial importance of considering the Pauli blocking in the present treatment. Disregarding the shell structure of the different A^{2+} ions, namely, allowing the electron to be captured to any state even if it is filled or empty, results in cross-section values that are higher by a factor of 2–10, depending on the ions and impact energies, than the ones obtained with inclusion of Pauli blocking.

In Fig. 5 the relative population of different subshells are plotted as a function of the projectile nuclear charge (Z_A) at the impact energies of 50 keV/amu and 1 MeV/amu. Comparing between the results at these two energies, the features due to two different collision mechanisms [2] are identified. At low impact energies the resonance condition, the smaller the difference between ϵ_i and ϵ_f the higher the probability of transfer, governs the process. The binding energies of the $B^{2+}(2s)$ and $C^{2+}(2p)$ states are nearly equal to the $1s$ orbital energy of the He atom. This feature is clearly seen in the figure, where a maximum population of the $n_f=2$ shell is realized at these ions. A similar peak can also be observed for the $n_f=3$ shell at around $Z_A=12$. However, the binding energies of the $n_f=3$ manifold reach the resonance condition for much heavier ions ($Z_A>14$), so the observed peak is considered to be formed by the increasing role of electron capture to the outer $n_f=4$ and $n_f=5$ shells with increasing Z_A and by the fact that the $n=2$ shell is fully occupied for the Mg^{2+} ion. A similar behavior of the relative population

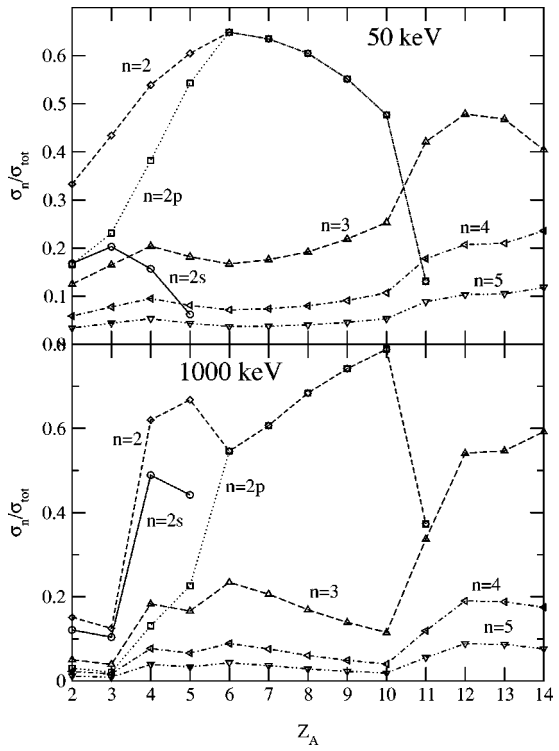

FIG. 5. Ratios of the partial σ_{nlm} to the total σ_{tot} electron capture cross sections in A^{2+}-He$(1s)\rightarrow A^{+}$-He$^{+}(1s)$ collisions calculated in the present CDW approximation.

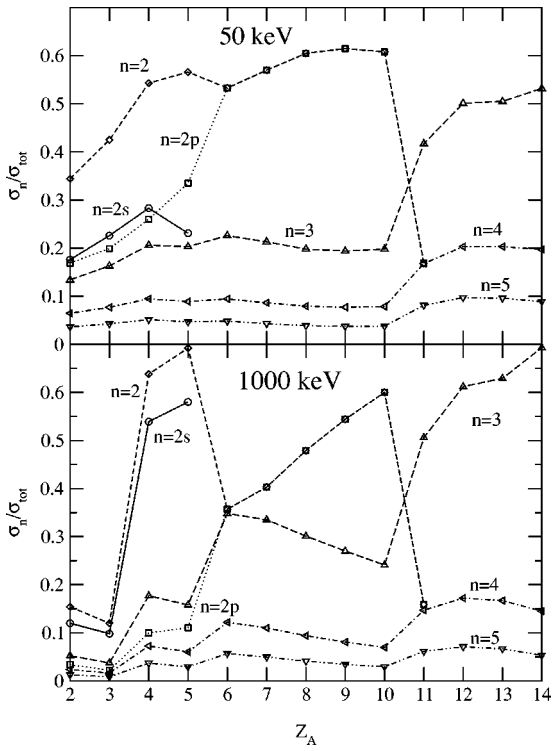

FIG. 6. Ratios of the partial σ_{nlm} to the total σ_{tot} electron capture cross sections in A^{2+}-He$(1s)\rightarrow A^{+}$-He$^{+}(1s)$ collisions calculated in the CDW approximation with Coulomb potential for the interaction of active electrons with the projectile ion (see the text).

of the different shells is no longer identified at high impact energy of 1 MeV/amu. Instead, the electron is predominantly captured into the innermost orbitals. This is characteristic of the fact that the matching between the initial and final momenta of the electron governs the mechanism. It is interesting to note that the relative population of a given orbital increases with Z_A and decreases suddenly at $Z_A=11$. The later is due to the fact that only one vacancy is available on the projectile ion.

The role of the ionic structure of the different A^{2+} ions can partly be considered in a theoretical treatment that is still based on approximating the projectile by Coulomb field, but with an effective charge q_{eff} defined by [1,3]

$$q_{eff}(nl)=[-2n^2\epsilon_f(nl)]^{1/2}. \tag{20}$$

We have also applied this (effective charge) method to the study of the A^{2+}-He collision. The binding energy (ϵ_f) for a given $n_f l_f$ final orbital was obtained using the potentials given by Sydlik and Green [17]. The wave function of He in the ground state was taken from Clementi and Roetti [15] and the distortion of the target ions (He^{+}) on the captured electron was set to be Coulombic. Actually, this is an application of the original extension of the CDW model to multielectron atoms by Belkić *et al.* [1,14], with the difference that the bare (Coulombic) projectile is described by Eq. (20). The effective charges (20) might differ appreciably for the different A^{2+} ions even for a given nl orbital, which is more realistic than using uniformly the net charge ($q=2$) [28]. This, including that the electron cannot be transferred to filled orbitals (Pauli blocking), already enables to consider characteristic of cross sections due to the different electronic shell structures of A^{2+} ions. The respective cross sections thus calculated with Eq. (20) and with Pauli blocking for the doubly charged ions obviously depend on each ionic species and deviate within a factor 2–5 from the predictions plotted in Fig. 4, which are based on describing the projectile field by a model potential.

Figure 6 illustrates the relative population of the different final states obtained from the above effective charge model. The peak structures characteristic for the resonant collision mechanism are not as emphasized on these results at 50 keV/amu as they are in Fig. 5. Moreover, the difference between the results at 50 keV/amu and 1 MeV/amu (Fig. 6) is not so appreciable, which is due to the fact that the dressed ions have been described as bare projectiles with appropriate Coulomb fields. In the case of bare projectile ions and at high impact energies it is well known that the capture cross section in the CDW model exhibits the Z_A^3 dependence on the projectile charge [3]. Such a strong dependence of capture cross section on Z_A can clearly be seen in the results at 1-MeV/amu impact energy in Fig. 5. Considering the binding energies of the different $n_f l_f$ orbitals the following tendencies can be observed for effective charges (20): at small value of $Z_A \leqslant 7$; $q_{eff}(2s)>q_{eff}(3s)>q_{eff}(2p)>q_{eff}(3p)$, while for the larger values of Z_A; $q_{eff}(2s)>q_{eff}(2p)>q_{eff}(3s)>q_{eff}(3p)$. This tendency and the strong Z_A^3 dependence explains why the relative population of the $n_f=3$ levels (dominated by the $3s$ orbital) exceeds that of $2p$ or-

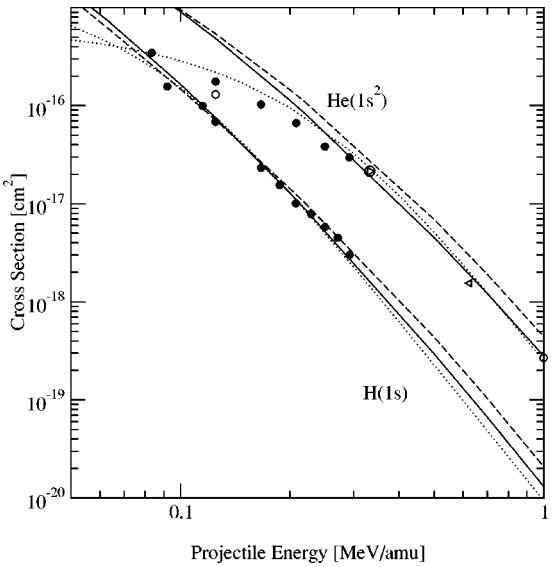

FIG. 7. Single-electron capture cross sections in A^{3+}-H(1s), He(1s)$\rightarrow A^{2+}$-H$^+$, He$^+$(1s) collisions. Solid and dashed lines are present results, respectively, for C^{3+} and O^{3+} projectiles; dotted line, recommended values obtained by semiempirical formula [27]. Symbols are the experimental data: ●, C^{3+}-H,He [30,31]; ▷, C^{3+}-He [32]; ○, O^{3+}-He [33]; ◁, O^{3+}-He [34].

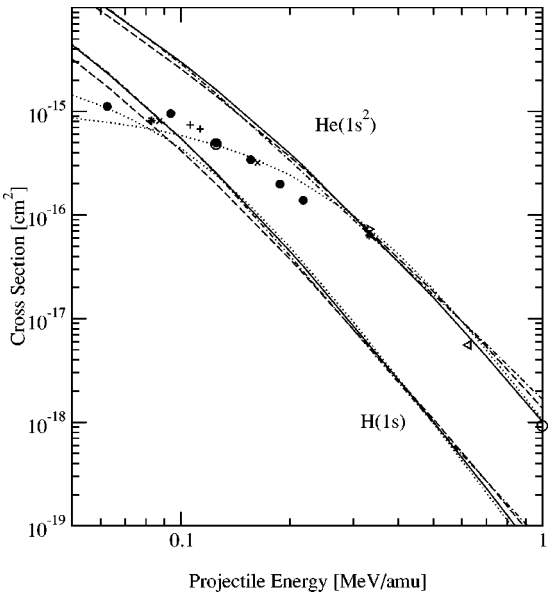

FIG. 8. Single electron capture cross sections in A^{5+}-H(1s), He(1s)$\rightarrow A^{4+}$-H$^+$, He$^+$(1s) collisions. Solid, dashed, and dot-dashed lines are present results, respectively, for O^{5+}, Ne^{5+}, and Si^{5+} projectiles; dotted lines, recommended values obtained by semiempirical formula [27]. Symbols are the experimental data: ●, O^{5+}-He [30]; ▷, O^{5+}-He [32]; ×, Ne^{5+}-He [32]; ○, O^{5+}-He [33]; ◁, O^{5+}-He [34]; +, O^{5+}-He [35]; ⋆, Ne^{5+}-He [36].

bital at low Z_A, and why it is below at medium or high values of Z_A. Such strong characteristic q_{eff}^3 dependence can be observed even at lower impact energies (50 keV/amu). Note that the relative population of the $n_f=2$ level does not clearly show a peak: $\sigma_{n_f=2}$ increase monotonically according to the monotonic increase of q_{eff} with increasing Z_A. Another remarkable difference between the results in Figs. 5 and 6 may be due to the Stark mixing between the s and p orbitals in the $n_f=2$ manifold [2]. The mixing is stronger in case of the present treatment, see Fig. 5, because the projectile orbitals have been described by a more realistic model potential.

2. $A^{3+,5+}$-He collision

Single electron capture cross sections of threefold and fivefold charged positive ions incident on the H and He atoms are presented in Figs. 7 and 8. In these figures are plotted the present results for some projectile ions along with the recommended data set based on a semiempirical formula [27] and the recent experimental data for C^{3+} and O^{5+} from [30,31].

In the case of $q=5$ projectiles the present calculated results are nearly independent of the ionic species compared with those for doubly charged ions in Fig. 4. This happens because the process becomes less sensitive to the electronic structure of the projectile ion as q increases [2,29]. At low impact energies around 50 keV/amu the electron is captured with high probability into the $n_f=3$ and $n_f=4$ levels of the fivefold charged ions. Considering the binding energies of these levels and the validity criteria of the CDW approximation (see above), the CDW model is expected to predict accurate cross-section values above (150–200)-keV/amu impact energies for both the H and He targets. Similar consideration predict a somewhat lower bound (100–150 keV/amu) for the applicability of the model in the case of triply charged projectiles. The validity of the CDW in the impact energy range estimated above seems to be confirmed by comparing with the experiments for C^{3+} and O^{5+} impinging on He [30,31], although the present theory still overestimates the data in the energy range below 200 keV/amu. In order to analyze these processes in more detail, more and new experiments would be very useful, especially, at high energies.

IV. CONCLUSION

We have extended the CDW model to treat the single electron capture processes in collisions of bare and dressed projectile ions with atoms and ions. The interactions of the active electron with both the projectile ion and the target are taken into account by means of model potentials.

In the case of proton incident on He, the present calculations for electron transfer to nonsymmetric Rydberg states shows better agreement with the experiment than the previous ones based on Coulomb distortion of the final captured state by the residual-target ion. The improvement is due to the better account of differential scattering cross section at projectile scattering angles characteristic of electron double scattering.

Calculated cross sections for single electron capture in the collisions of multiply-charged dressed ions ($q=2,3,5$) with He show that the capture mechanism becomes less sensitive to the electronic structure of the projectile with increasing q. The relative population of different final orbitals has been analyzed in the case of doubly charged projectile ions and characteristic features of different collision mechanism based on energy resonance and momentum transfer have been observed in the low and high impact energy regions, respectively. These features are less apparent when the interaction between the projectile ion and active electron is replaced with a screened Coulomb field that gives a less accurate description of the final orbitals and overemphasizes the distortion.

ACKNOWLEDGMENTS

We thank R. Janev and A. Salin for helpful discussions. This work was partially supported by the Science and Technology Agency of Japan. L.G. and P.D.F. acknowledge financial support from the International Atomic Energy Agency (Contract No. 10084/RO) and from the Hungarian-Argentinean Intergovernmental S&T Cooperation Program (SCyT-OMFB HUN4/99/OG). L. G. gratefully acknowledges the financial support of the Bolyai Research Foundation of the Hungarian Academy of Sciences. P.D.F. acknowledges the hospitality at the ATOMKI and financial support from Agencia Nacional de Promoción Científica y Tecnológica (Grant No. 03-04021).

[1] Dž. Belkić, R. Gayet, and A. Salin, Phys. Rep. **56**, 249 (1979).
[2] R.K. Janev, L.P. Presnyakov, and V.P. Shevelko, *Physics of Highly Charged Ions* (Springer-Verlag, Berlin, 1985).
[3] D.P. Dewangan and J. Eichler, Phys. Rep. **247**, 59 (1994).
[4] J.H. McGuire, *Electron Correlation Dynamics in Atomic Collisions* (Cambridge University Press, Cambridge, 1997).
[5] Dž. Belkić, R. Gayet, J. Hanssen, I. Mančev, and A. Nunez, Phys. Rev. A **56**, 3675 (1997).
[6] I. Mančev, Phys. Rev. A **60**, 351 (1999).
[7] Dž. Belkić, J. Comp. Math. Sci. Eng. **1**, 1 (2001).
[8] I.M. Cheshire, Proc. Phys. Soc. London **84**, 89 (1964).
[9] R. Gayet, J. Phys. B **5**, 483 (1972).
[10] D.S.F. Crothers and L. Dubé, Adv. At., Mol., Opt. Phys. **30**, 285 (1993).
[11] L. Gulyás, P.D. Fainstein, and A. Salin, J. Phys. B **28**, 245 (1995).
[12] L. Gulyás and P.D. Fainstein, Phys. Rev. A **56**, 1321 (1997).
[13] H. Bachau, G.R. Deco, and A. Salin, J. Phys. B **21**, 1403 (1988).
[14] Dž. Belkić, R. Gayet, and A. Salin, Comput. Phys. Commun. **32**, 385 (1979).
[15] E. Clementi and C. Roetti, At. Data Nucl. Data Tables **14**, 177 (1974).
[16] F. Herman and S. Skillman, *Atomic Structure Calculations* (Prentice-Hall, Inc., Englewood Cliffs, NJ, 1963).
[17] P.P. Szydlik and A.E.S. Green, Phys. Rev. A **9**, 1885 (1974).
[18] J.R.S. Crisholm, A. Genz, E. Clengs, and E. Rowlands, I. Comput. Phys. **10**, 284 (1972).
[19] Dž. Belkić, R. Gayet, and A. Salin, At. Data Nucl. Data Tables **51**, 59 (1992).
[20] S. Suzuki, L. Gulyás, N. Shimakura, P.D. Fainstein, and T. Shirai, J. Phys. B **33**, 3307 (2000).
[21] M.B. Shah and H.B. Gilbody, J. Phys. B **18**, 899 (1985).
[22] J. Burgdörfer and L.J. Dubé, Phys. Rev. A **31**, 634 (1985).
[23] R.D. Rivarola and J.E. Miraglia, J. Phys. B **15**, 2221 (1982).
[24] D.S.F. Crothers and J.F. McCann, J. Phys. B **17**, l177 (1984).
[25] R. Hoekstra, H.P. Summers, and F.J. de Heer, Suppl. J. Nucl. Fusion **3**, 63 (1992).
[26] R. Ito, T. Tabata, T. Shirai, and R.A. Phaneuf, Japan Atomic Energy Research Institute, Report No. JAERI-M 93-117, 1993 (unpublished).
[27] Y. Nakai, T. Shirai, T. Tabata, and R. Ito, Phys. Scr. **T28**, 77 (1989).
[28] Dž. Belkić, Phys. Scr. **43**, 561 (1991).
[29] C. Illescas and A. Riera, Phys. Rev. A **60**, 4546 (1999).
[30] W.S. Melo, M.M. Sant'Anna, A.C.E. Santos, G.M. Sigaud, and E.C. Montenegro, Phys. Rev. A **60**, 1124 (1999).
[31] M.M. Sant'Anna, W.S. Melo, A.C.E. Santos, M.B. Shah, G.M. Sigaud, and E.C. Montenegro, J. Phys. B **33**, 353 (2000).
[32] V. Nikolaev *et al.*, Sov. Phys. JETP **13**, 695 (1961).
[33] H. Knudsen *et al.*, Phys. Rev. A **23**, 597 (1981).
[34] V. Macdonald and M. Martin, Phys. Rev. A **4**, 1965 (1971).
[35] J.E. Bayfield *et al.*, Rev. Sci. Instrum. **51**, 651 (1980).
[36] N. Dmitriev *et al.*, Sov. Phys. JETP **46**, 884 (1977).